Contents lists available at Science-Gate

International Journal of Advanced and Applied Sciences

Journal homepage: http://www.science-gate.com/IJAAS.html

Modeling COVID-19 mortality data in four countries using odd generalized exponential Kumaraswamy-Inverse exponential distribution

Lamya A. Baharith *

Department of Statistics, Faculty of Science, King Abdulaziz University, Jeddah, Saudi Arabia

ARTICLE INFO

Article history:
Received 3 January 2022
Received in revised form
24 March 2022
Accepted 20 April 2022

Keywords:
Odd generalized exponential generator
Kumaraswamy generalized family
Inverse-exponential distribution
COVID-19 data

ABSTRACT

This study aims to introduce an optimum model to assess the COVID-19 death rate in Saudi Arabia, Canada, Italy, and Mexico. A novel five-parameter lifetime distribution termed the odd generalized exponential Kumaraswamy-inverse exponential distribution is presented by combining the Kumaraswamy-inverse exponential distribution with the odd generalized exponential generator. The theoretical features of the new distribution, as well as its reliability functions, moments, and order statistics are investigated. The odd generalized exponential Kumaraswamy-inverse exponential distribution is of special importance since its density has a variety of symmetric and asymmetric forms. Furthermore, the graphs of the hazard rate function exhibit various asymmetrical shapes such as decreasing, increasing, and upside-down bathtub shapes, and inverted J-shapes making The odd generalized exponential Kumaraswamy-inverse exponential distribution suitable for modeling hazards behaviors more likely to be observed in practical settings like human mortality, and biological applications. The proposed distribution parameters are estimated using the maximum likelihood approach and its effectiveness is demonstrated through both numerical study and applications to four COVID-19 mortality rate data sets. The odd generalized exponential Kumaraswamy-inverse exponential distribution provides the best fit to COVID-19 data compared to other extended forms of the Kumaraswamy and inverse exponential distributions which may attract wider applications in different fields.

1. Introduction

Severe acute respiratory syndrome coronavirus 2 (SARS-CoV-2) was discovered during the recent pneumonia epidemic in January 2020 in Wuhan, China. Ever since, the virus has rapidly spread around the world, infecting many people and causing severe pneumonia with a high mortality rate. This has forced many governments to take exceptional actions to safeguard their citizens. Therefore, several researchers proposed various new statistical models to accurately fit the COVID-19 data, see for example Almongy et al. (2021), Almetwally et al. (2021), Bantan et al. (2020), and Mohamed et al. (2021).

There are still numerous real-world issues where actual data does not fit any of the well-known probability models. In order to address this, there is a significant need to develop probability models that better reflect the behavior of particular real-life phenomena.

Generated families of continuous distributions are a recent invention that offers a great deal of versatility in modeling real-world data. The addition of new parameter(s) to established distributions enhance their appropriateness for real-life phenomenon and increase the accuracy of characterizing the shape of the distribution's tail. A number of families were generated in previous studies using new approaches, for example, the beta-G family by Eugene et al. (2002), the Kumaraswamy-G family (kum-G) by Cordeiro and de Castro (2011), and the more general method T-X family introduced by Alzaatreh et al. (2013) which allowed any continuous distribution to be the generator, Weibull-G by Bourguignon et al. (2014), exponentiated Weibull-G by Cordeiro et al. (2017), odd generalized exponential-G (OEG) by Tahir et al. (2015), among many others.

Our focus here is on the OEG family, which is versatile due to its different hazard rate shape properties. The OEG family is useful for evaluating

* Corresponding Author.
Email Address: lbaharith@kau.edu.sa
https://doi.org/10.21833/ijaas.2022.07.011
Corresponding author's ORCID profile:
https://orcid.org/0000-0001-8070-956X

many types of lifespan data. If G(x) is any continuous cumulative distribution function (CDF), then the CDF and the probability density function (pdf) of the OEG family can be expressed, respectively, as:

$$F_{OEG}(x;\alpha,\lambda)=\left(1-e^{-\lambda\frac{G(x)}{1-G(x)}}\right)^{\alpha},\quad x>0;\alpha,\lambda>0, \tag{1}$$

$$f_{OEG}(x;\alpha,\lambda)=\frac{\lambda\alpha g(x)}{[1-G(x)]^2}e^{-\lambda\frac{G(x)}{1-G(x)}}\left(1-e^{-\lambda\frac{G(x)}{1-G(x)}}\right)^{\alpha-1},\quad x>0;\ \alpha,\lambda>0. \tag{2}$$

The exponential distribution is a well-known model in life testing studies due to its straightforward mathematical application and intriguing characteristics. As a result, it has been generalized by a number of scholars. However, the exponential distribution has a major drawback in that it has bad memory characteristics and a constant failure rate, which is inappropriate for modeling specific cases with bathtub and inverted bathtub failure rates (Lemonte, 2013). Therefore, a modified version of the exponential distribution, named inverse exponential distribution (IE), is proposed and studied by Keller et al. (1982) and Lin et al. (1989) to compensate for these constraints. The CDF and pdf of IE distribution are expressed, respectively, as:

$$F_{IE}(x;\gamma)=e^{-\frac{\gamma}{x}},\quad x>0;\ \gamma>0, \tag{3}$$

$$f_{IE}(x;\gamma)=\frac{\gamma}{x^2}e^{-\frac{\gamma}{x}},\quad x>0;\ \gamma>0. \tag{4}$$

Various generalizations of the IE distribution have been contributed in recent years to improve its flexibility, including the generalized inverted exponential by Abouammoh and Alshingiti (2009), the exponentiated generalized inverse-exponential (Oguntunde et al., 2014), the Odd generalized exponential inverse-exponential (Yahaya and Abba, 2017), and the exponentiated transmuted inverse-exponential (Mohammed and Yahaya, 2019).

The Kumaraswamy distribution has recently gained popularity due to its attractable representations for its CDF, pdf, and moments. Furthermore, it is widely used in hydrology applications (Cordeiro and de Castro, 2011; Jones, 2009; Kumaraswamy, 1980).

As a result of the appealing properties and potentials of both the Kumaraswamy and IE distributions, the Kum-G family is employed by Mohammed and Yahaya (2019) and Oguntunde et al. (2017) to generate the Kumaraswamy-IE (Kum-IE) distribution with CDF as follow:

$$G_{Kum-IE}(x;a,\beta,\gamma)=1-\left[1-e^{-\frac{a\gamma}{x}}\right]^{\beta},\quad x>0;a,\beta,\gamma>0. \tag{5}$$

The associated pdf of Eq. 5 is given as:

$$g_{Kum-IE}(x;a,\beta,\gamma)=\gamma a\beta x^{-2}e^{-\frac{a\gamma}{x}}\left[1-e^{-\frac{a\gamma}{x}}\right]^{\beta-1},\ x>0;a,\beta,\gamma>0. \tag{6}$$

This study aims to suggest a novel lifetime distribution termed the Odd generalized exponential Kumaraswamy-inverse exponential (OEKIE) distribution, based on a previous study's odd generalized exponential generator, T-X, and Kum-G family. Furthermore, the following are the major reasons for implementing OEKIE in practice:

- Provides additional adaptability for modeling real-world data in a variety of disciplines by combining the OEG, T-X, and Kum-G approaches for generating new distributions.
- Provides an appropriate model for fitting COVID-19 mortality rate data.
- Improve the flexibility of the Kum-IE distribution by providing new generalizations.
- Provides more diverse lifetime data fits than its rival.

In this article, some of OEKIE's theoretical properties are deduced in Section 2, with an emphasis on those that may be of broad importance in probability and statistics. The maximum likelihood (ML) approach is adopted to estimate the OEKIE's parameters in Section 3. In Section 4, a numerical study is carried out. Section 5 presents different COVID-19 mortality rate data sets from four countries to demonstrate the efficiency of the OEKIE distribution in comparison to some competitive generalized distributions of IE and Kumaraswamy. Finally, concluding remarks are provided in Section 6.

2. The OEKIE distribution

The CDF and pdf of OEKIE can be obtained by replacing the $G(x)$ and $g(x)$ in (1) and (2) by (5) and (6) as follows:

$$F(x;\alpha,\lambda,a,\beta,\gamma)=\left[1-e^{-\lambda\left(\left[1-e^{-\frac{a\gamma}{x}}\right]^{-\beta}-1\right)}\right]^{\alpha},\ x>0;\alpha,\lambda,a,\beta,\gamma>0, \tag{7}$$

and

$$f(x;\alpha,\lambda,a,\beta,\gamma)=\frac{\lambda\alpha\gamma a\beta\left(e^{-\frac{\gamma}{x}}\right)^{a}}{x^2\left[1-e^{-\frac{a\gamma}{x}}\right]^{\beta+1}}\ e^{-\lambda\left(\left[1-\left(e^{-\frac{\gamma}{x}}\right)^{a}\right]^{-\beta}-1\right)}\left[1-e^{-\lambda\left(\left[1-e^{-\frac{a\gamma}{x}}\right]^{-\beta}-1\right)}\right]^{\alpha-1},\ x>0;\alpha,\lambda,a,\beta,\gamma>0. \tag{8}$$

The Survival function, $S(x)$, and hazard rate function (hrf) of OEKIE are expressed as:

$$S(x;\alpha,\lambda,a,\beta,\gamma)=1-\left[1-e^{-\lambda\left(\left[1-e^{-\frac{a\gamma}{x}}\right]^{-\beta}-1\right)}\right]^{\alpha},\ x>0;\alpha,\lambda,a,\beta,\gamma>0, \tag{9}$$

$$h(x;\alpha,\lambda,a,\beta,\gamma)=\frac{\lambda\alpha\gamma a\beta\left(e^{-\frac{\gamma}{x}}\right)^{a}e^{-\lambda\left(\left[1-e^{-\frac{a\gamma}{x}}\right]^{-\beta}-1\right)}\left[1-e^{-\lambda\left(\left[1-e^{-\frac{a\gamma}{x}}\right]^{-\beta}-1\right)}\right]^{\alpha-1}}{x^{2}\left[1-e^{-\frac{a\gamma}{x}}\right]^{\beta+1}\left(1-\left[1-e^{-\lambda\left(\left[1-e^{-\frac{a\gamma}{x}}\right]^{-\beta}-1\right)}\right]^{\alpha}\right)},\ x>0;\alpha,\lambda,a,\beta,\gamma>0. \quad (10)$$

Fig. 1 and Fig. 2 show the various forms of OEKIE's density and hrf at some values of the parameters. The pdf of the OEKIE in Fig. 1 shows decreasing, symmetrical, right-skewed, and reversed J-shape, which demonstrates the various modeling scenarios. In addition, the OEKIE's hrf is attractive as seen in Fig. 2 since it exhibits a wide range of asymmetrical forms, including increasing, bath-tab, decreasing, constant, and reversed J-shape. This diverse panel of shapes reflects OEKIE's flexibility.

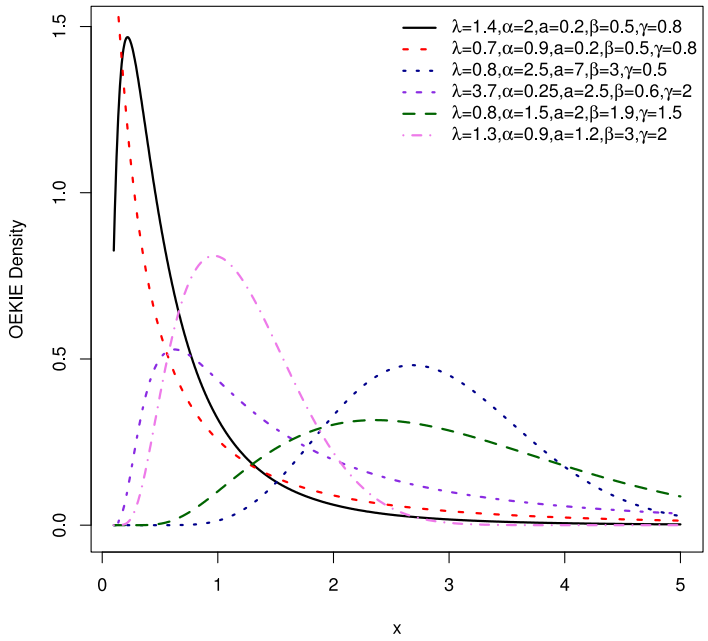

Fig. 1: The plots for the OEKIE pdf for certain values

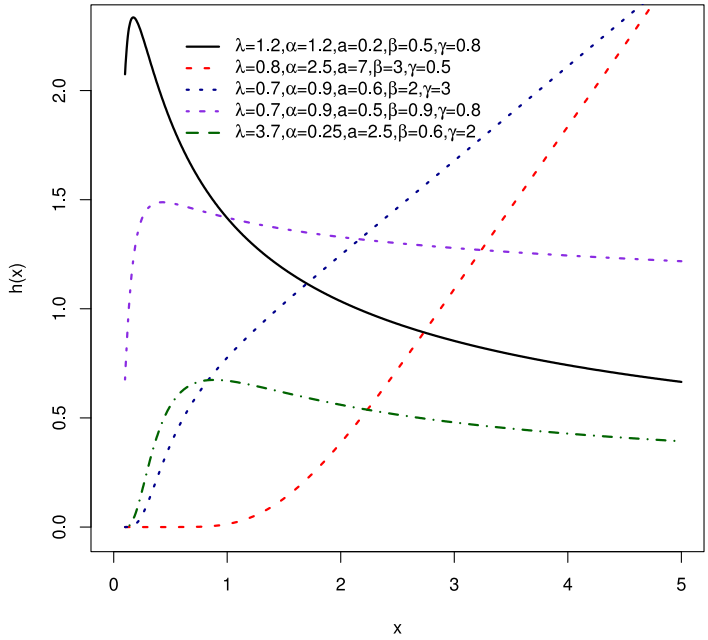

Fig. 2: The OEKIE's hrf plots at some selected values

2.1. Alternative expression for OEKIE's density

This subsection provides expansion for the OEKIE's pdf given in Eq. 8 by first considering the binomial theorem series defined by,

$$(1-z)^{a}=\sum_{d=0}^{\infty}(-1)^{d}\binom{a}{d}z^{d}. \quad (11)$$

In addition, the expansion of the exponential function is defined as:

$$e^{-x} = \sum_{i=0}^{\infty} \frac{(-1)^i}{i!} x^i. \quad (12)$$

Employing Eq. 11 to expand $\left[1 - e^{-\lambda\left(\left[1-e^{-\frac{a\gamma}{x}}\right]^{-\beta}-1\right)}\right]^{\alpha-1}$, the OEKIE's pdf in Eq. 8 will be rewritten as:

$$f(x) = \frac{\alpha\gamma a\beta e^{-\frac{a\gamma}{x}}}{x^2} \sum_{j_1=0}^{\infty} \sum_{j_2=0}^{\infty} \frac{(-1)^{j_1+j_2} \lambda^{j_2+1} (j_1+1)^{j_2}}{j_2! \left[1-e^{-\frac{a\gamma}{x}}\right]^{\beta j_2+\beta+1}} \binom{\alpha-1}{j_1} \left(1 - \left[1-e^{-\frac{a\gamma}{x}}\right]^{-\beta}\right)^{j_2}.$$

Additionally, by employing Eq. 11 twice, the pdf of OEKIE will reduce to

$$f(x) = \alpha\gamma a\beta \sum_{j_4=0}^{\infty} \frac{\eta_{j_4} \lambda^{j_2+1}}{x^2} e^{-\frac{aj_4\gamma}{x}}, \quad (13)$$

where,

$$\eta_{j_4} = \sum_{j_1=0}^{\infty} \sum_{j_2=0}^{\infty} \sum_{j_3=0}^{j_2} \frac{(-1)^{j_1+j_2+j_3+j_4} (j_1+1)^{j_2}}{j_2!} \binom{\alpha-1}{j_1} \binom{j_2}{j_3} \binom{\beta(j_3-j_2-1)-1}{j_4}. \quad (14)$$

3. Properties of the OEKIE

This section presents some essential statistical properties of OEKIE as follows:

3.1. Quantile function

The quantile function (x_p) of the OEKIE distribution can be expressed as:

$$x_p = -a\gamma \left\{\log\left[1 - \left(1 - \frac{\log(1-p^{1/\alpha})}{\lambda}\right)^{-1/\beta}\right]\right\}^{-1}, \quad 0 < p < 1. \quad (15)$$

Therefore, the OEKIE's median can be obtained as:

$$x_{0.50} = -a\gamma \left\{\log\left[1 - \left(1 - \frac{\log(1-p^{1/\alpha})}{\lambda}\right)^{-1/\beta}\right]\right\}^{-1}.$$

Hence, the 25^{th} and 75^{th} percentiles of the OEKIE are obtained from Eq. 15 by replacing p by (0.25,0.75), respectively.

3.2. Skewness and kurtosis

The shapes of OEKIE can be studied using Galton's skewness and Moors' kurtosis (Moors, 1988). This is easily obtained using Eq. 15, as follows:

$$Skewness = \frac{X_{0.75} - 2X_{0.5} + X_{0.25}}{X_{0.75} - X_{0.25}}, \quad (16)$$

and

$$Kurtosis = \frac{X_{0.875} - X_{0.625} + X_{0.375} - X_{0.125}}{X_{0.75} - X_{0.25}}. \quad (17)$$

For details see Alzaatreh et al. (2013). Fig. 3 and Fig. 4 display the Galton's skewness and Moors' kurtosis for OEKIE at different values of α, λ when $a = 2, \beta = 1.2, \gamma = 0.3$ and at different values of λ, γ when $a = 0.2, \beta = 1.2, \alpha = 1.3$. It can be seen that the skewness is always positive, implying that OEKIE is right-skewed. Fig. 3 shows that the kurtosis is a decreasing function of λ and α, but the Galton's skewness is increasing function of λ for fixed α and is decreasing function of α for fixed λ. Fig. 4 shows that kurtosis is increasing function of λ and skewness is decreasing function of γ.

3.3. Moments

If X has the OEKIE with density (8), then the r^{th} moment of X is given by,

$$E(x^r) = \int_0^{\infty} x^r f(x) dx = \alpha\gamma a\beta \sum_{j_4=0}^{\infty} \eta_{j_4} \lambda^{j_2+1} \int_0^{\infty} x^{r-2} e^{-\frac{aj_4\gamma}{x}} dx, \quad (18)$$

where, η_{j_4} given by Eq. 14. Taking $z = aj_4\gamma x^{-1}$, limits will change from ∞ to 0, then simplifying, we obtain:

$$E(x^r) = \alpha\gamma^r a^r \beta \sum_{j_4=0}^{\infty} \eta_{j_4} \lambda^{j_2+1} j_4^{r-1} \int_0^{\infty} z^{-r} e^{-z} dz.$$

Thus, the r^{th} moment is expressed as:

$$\mu_r = E(x^r) = \alpha\gamma^r a^r \beta \sum_{j_4=0}^{\infty} \eta_{j_4} \lambda^{j_2+1} j_4^{r-1} \Gamma(1-r), r < 1, \quad (19)$$

where, the gamma function is defined as:

$$\Gamma(\phi) = \int_0^{\infty} x^{\phi-1} e^{-x} dx. \quad (20)$$

The expression in Eq. 19 suggests that OEKIE's r^{th} the moment does not exist for $r \geq 1$.

3.4. Moment generating function

The OEKIE's moment generating function (MGF) is easily expressed as:

$$M_x(t) = E(e^{tx}) = \sum_{r=0}^{\infty} \frac{t^r}{r!}\mu_r = \alpha\beta \sum_{r=0}^{\infty} \sum_{j_4=0}^{\infty} \frac{t^r}{r!}\gamma^r a^r \eta_{j_4} \lambda^{j_2+1} j_4^{r-1}\Gamma(1-r), \quad (21)$$

where $r \geq 1$ and η_{j_4} is given by Eq. 14.

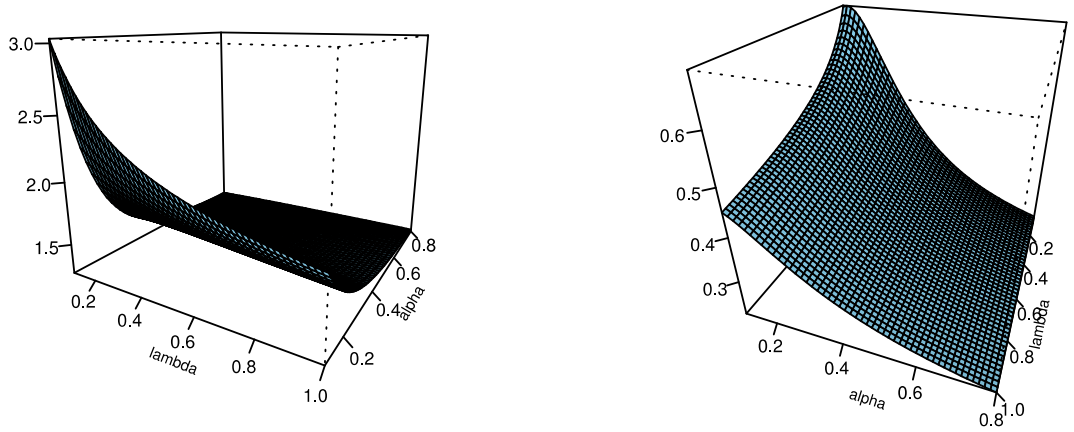

Moors-Kurtosis **Galton-Skewness**

Fig. 3: OEKIE's Skewness and Kurtosis plots for various values of α and λ

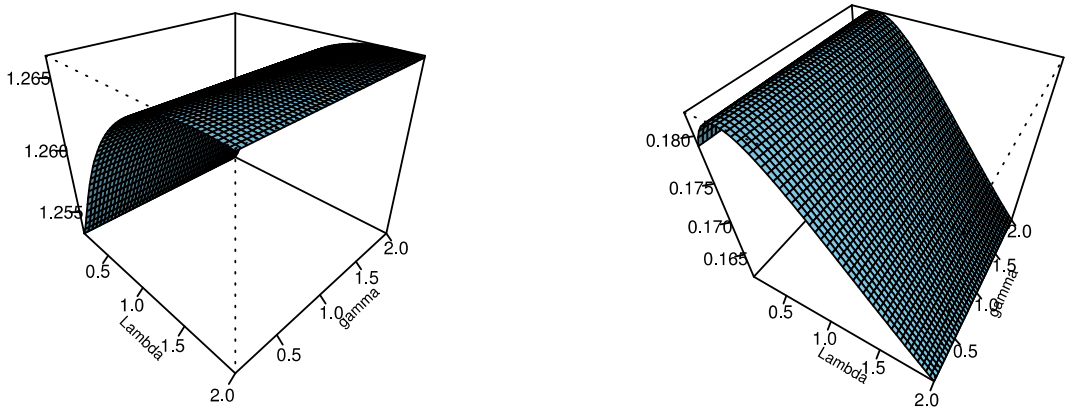

Moors-Kurtosis **Galton-Skewness**

Fig. 4: OEKIE's Skewness and Kurtosis plots for various values of λ and γ

3.5. Characteristic function

The OEKIE's characteristic function is easily obtained as follows:

$$\phi_x(t) = E(e^{itx}) = \alpha\beta \sum_{r=0}^{\infty} \sum_{j_4=0}^{\infty} \frac{(it)^r}{r!}\gamma^r a^r \eta_{j_4} \lambda^{j_2+1} j_4^{r-1}\Gamma(1-r), \quad (22)$$

where $r \geq 1$ and η_{j_4} is given by 14.

3.6. Rényi entropy

The level of uncertainty of an R.V. X having pdf $f(x)$ is defined by its entropy. The Rényi entropy, denoted by $(RE_X(\nu))$, is formulated as:

$$RE_X(\nu) = \frac{1}{1-\nu}\log\left(\int_0^{\infty} f(x)^{\nu} dx\right); \quad \nu > 0, \nu \neq 1.$$

Therefore, using the pdf of OEKIE in (8), $f(x)^{\nu}$ is expressed as:

$$f^{\nu}(x) = \left(\frac{\lambda\alpha\gamma a\beta e^{-\frac{a\gamma}{x}}}{x^2\left[1-e^{-\frac{a\gamma}{x}}\right]^{(\beta+1)}}\right)^{\nu}\left[e^{-\lambda\left(\left[1-e^{-\frac{a\gamma}{x}}\right]^{-\beta}-1\right)}\right]^{\nu}\left[1-e^{-\lambda\left(\left[1-e^{-\frac{a\gamma}{x}}\right]^{-\beta}-1\right)}\right]^{\nu(\alpha-1)}.$$

Applying the same approach in Subsection 1.1 and using Eq. 11, then:

$$f^{\nu}(x) = \left(\frac{\lambda\alpha\gamma a\beta e^{-\frac{a\gamma}{x}}}{x^2\left[1-e^{-\frac{a\gamma}{x}}\right]^{(\beta+1)}}\right)^{\nu}\sum_{j_1=0}^{\infty}(-1)^{j_1}\binom{\nu(\alpha-1)}{j_1}\left[e^{-\lambda(\nu+j_1)\left(\left[1-e^{-\frac{a\gamma}{x}}\right]^{-\beta}-1\right)}\right].$$

Using Eq. 12 to expand $\left[e^{-\lambda(v+j_1)\left(\left[1-e^{-\frac{a\gamma}{x}}\right]^{-\beta}-1\right)}\right]$, then,

$$f^v(x)=(\alpha\gamma a\beta)^v\sum_{j_1=0}^{\infty}sum_{j_2=0}^{\infty}\frac{(-1)^{j_1+j_2}\lambda^{j_2+1}(v+j_1)^{j_2}}{x^{2v}j_2!}\binom{v(\alpha-1)}{j_1}\left(e^{-\frac{a\gamma}{x}}\right)^v\times\left[1-e^{-\frac{a\gamma}{x}}\right]^{-v(\beta+1)-j_2\beta}\left(1-\left[1-e^{-\frac{a\gamma}{x}}\right]^{\beta}\right)^{j_2}.$$

Additionally, by employing Eq. 11 to expand $\left(1-\left[1-e^{-\frac{a\gamma}{x}}\right]^{\beta}\right)^{j_2}$, then:

$$f^v(x)=(\alpha\gamma a\beta)^v\sum_{j_1=0}^{\infty}\sum_{j_2=0}^{\infty}\sum_{j_3=0}^{j_2}\frac{(-1)^{j_1+j_2+j_3}\lambda^{j_2+1}(v+j_1)^{j_2}}{x^{2v}j_2!}\binom{v(\alpha-1)}{j_1}\binom{j_2}{j_3}\times\left(e^{-\frac{\gamma}{x}}\right)^{av}\left[1-e^{-\frac{a\gamma}{x}}\right]^{j_3\beta-v(\beta+1)-j_2\beta}.$$

Finally, employing Eq. 11 to expand $\left[1-e^{-\frac{a\gamma}{x}}\right]^{j_3\beta-v(\beta+1)-j_2\beta}$, then $f(x)^v$ will be reduced to:

$$f^v(x)=(\alpha\gamma a\beta)^v\sum_{j_4=0}^{\infty}\eta_{j_4}^*x^{-2v}\left(e^{-\frac{\gamma}{x}}\right)^{av+aj_4},$$

where,

$$\eta_{j_4}^*=\sum_{j_1=0}^{\infty}\sum_{j_2=0}^{\infty}\sum_{j_3=0}^{j_2}\frac{(-1)^{j_1+j_2+j_3}j_2!\,\lambda^{j_2+1}(v+j_1)^{j_2}}{j_2!}\binom{v(\alpha-1)}{j_1}\binom{j_2}{j_3}\binom{\beta(j_3-j_2-v)-v}{j_4}.$$

By setting $u=a\gamma(v+j_4)x^{-1}$, the Rényi entropy of the OEKIE, is given by:

$$RE_x(v)=\frac{1}{1-v}\log[(\alpha\beta)^v(\gamma a)^{-(v+1)}\sum_{j_4=0}^{\infty}\eta_{j_4}^*\Gamma(1-2(v+1))],\quad 2(v+1)<1.$$

3.7. Order statistics

Suppose $X_1,X_2,\ldots\ldots,X_n$ is a random sample (R.S.) from OEKIE and $X_{s:n}$ denotes the s^{th} order statistics. Therefore, the pdf, $f_{s:n}(x)$, of the s^{th} order statistics are expressed as:

$$f_{s:n}(x)=\frac{n!}{(s-1)!(n-s)!}f(x)[F(x)]^{s-1}[1-F(x)]^{n-s}. \quad (23)$$

Applying the binomial series expansion of Eq. 11 to Eq. 23, $f_{s:n}(x)$ will be,

$$f_{s:n}(x)=\frac{n!}{(s-1)!(n-s)!}f(x)\sum_{k=0}^{\infty}(-1)^k\binom{n-s}{k}[F(x)]^{k+s-1}.$$

(24)

By substituting the CDF of OEKIE into (24), the pdf of $X_{s:n}$ is:

$$f_{s:n}(x)=\frac{n!\,f(x)}{(s-1)!\,(n-s)!}\sum_{k=0}^{\infty}(-1)^k\binom{n-s}{k}\left[1-e^{-\lambda\left(\left[1-e^{-\frac{a\gamma}{x}}\right]^{-\beta}-1\right)}\right]^{\alpha(k+s-1)},$$

where f(x) is the OEKIE's pdf given by (8).

4. ML estimation

Let $x_1,\ldots,x_n$ be a R.S. of size n from OEKIE. The log-likelihood function, (ℓ), for $\Theta=(\lambda,\alpha,a,\beta,\gamma)$, is given by,

$$\ell(\Theta)=n\log(\lambda\alpha\gamma a\beta)-2\sum_{i=1}^{n}\log(x_i)-a\sum_{i=1}^{n}\frac{\gamma}{x_i}-(\beta+1)\sum_{i=1}^{n}\log\left[1-e^{-\frac{a\gamma}{x}}\right]-\lambda\sum_{i=1}^{n}\left(\left[1-e^{-\frac{a\gamma}{x}}\right]^{-\beta}-1\right)+(\alpha-1)\sum_{i=1}^{n}\log\left[1-e^{-\lambda\left(\left[1-e^{-\frac{a\gamma}{x}}\right]^{-\beta}-1\right)}\right]. \quad (25)$$

Therefore, the ML estimates (MLEs) of the parameters can be computed via maximizing Eq. 25. That is, the first derivative of Eq. 25 with respect to λ,α,a,β, and γ are as follows:

$$\frac{\partial\ell}{\partial\lambda}=\frac{n}{\lambda}-\sum_{i=1}^{n}\left(\left(1-e^{-\frac{a\gamma}{x_i}}\right)^{\beta}-1\right)-(\alpha-1)\sum_{i=1}^{n}\frac{\left(1-\left(1-e^{-\frac{a\gamma}{x_i}}\right)^{-\beta}\right)e^{-\lambda\left(\left(1-e^{-\frac{a\gamma}{x_i}}\right)^{-\beta}-1\right)}}{1-e^{-\lambda\left(\left(1-e^{-\frac{a\gamma}{x_i}}\right)^{-\beta}-1\right)}},$$

$$\frac{\partial \ell}{\partial \alpha} = \frac{n}{\alpha} + \log \sum_{i=1}^{n} \left(1 - e^{-\lambda \left(\left(1 - e^{-\frac{a\gamma}{x_i}} \right)^{-\beta} - 1 \right)} \right),$$

$$\frac{\partial \ell}{\partial a} = \frac{n}{a} - \sum_{i=1}^{n} \frac{\gamma}{x_i} - (\beta + 1)\gamma \sum_{i=1}^{n} \frac{e^{-\frac{a\gamma}{x_i}}}{x_i \left(1 - e^{-\frac{\gamma a}{x_i}} \right)} + \beta\gamma\lambda \sum_{i=1}^{n} \frac{e^{-\frac{a\gamma}{x_i}} \left(1 - e^{-\frac{a\gamma}{x_i}} \right)^{-\beta-1}}{x_i}$$

$$- \beta\gamma\lambda(\alpha - 1) \sum_{i=1}^{n} \frac{e^{-\frac{a\gamma}{x_i}} \left(1 - e^{-\frac{a\gamma}{x_i}} \right)^{-\beta-1} e^{-\lambda \left(\left(1 - e^{-\frac{a\gamma}{x_i}} \right)^{-\beta} - 1 \right)}}{x_i \left(1 - e^{-\lambda \left(\left(1 - e^{-\frac{a\gamma}{x_i}} \right)^{-\beta} - 1 \right)} \right)},$$

$$\frac{\partial \ell}{\partial \beta} = \frac{n}{\beta} - \log \sum_{i=1}^{n} \left(1 - e^{-\frac{a\gamma}{x_i}} \right) + \lambda \sum_{i=1}^{n} \frac{\log \left(1 - e^{-\frac{a\gamma}{x_i}} \right)}{\left(1 - e^{-\frac{a\gamma}{x_i}} \right)^{\beta}} - \lambda(\alpha - 1) \sum_{i=1}^{n} \frac{\log \left(1 - e^{-\frac{a\gamma}{x_i}} \right) e^{-\lambda \left(\left(1 - e^{-\frac{a\gamma}{x_i}} \right)^{\beta-1} - 1 \right)}}{\left(1 - e^{-\frac{a\gamma}{x_i}} \right)^{\beta} \left(1 - e^{-\lambda \left(\left(1 - e^{-\frac{a\gamma}{x_i}} \right)^{\beta-1} - 1 \right)} \right)}$$

$$\frac{\partial \ell}{\partial \gamma} = \frac{n}{\gamma} - \sum_{i=1}^{n} \frac{a}{x_i} - a(\beta + 1) \sum_{i=1}^{n} \frac{e^{-\frac{a\gamma}{x_i}}}{x_i \left(1 - e^{-\frac{a\gamma}{x_i}} \right)} + a\beta\lambda \sum_{i=1}^{n} \frac{\left(1 - e^{-\frac{a\gamma}{x_i}} \right)^{-\beta-1} e^{-\frac{a\gamma}{x_i}}}{x_i}$$

$$- a\beta\lambda(\alpha - 1) \sum_{i=1}^{n} \frac{e^{-\frac{a\gamma}{x_i}} \left(1 - e^{-\frac{a\gamma}{x_i}} \right)^{-\beta-1} e^{-\lambda \left(\left(1 - e^{-\frac{a\gamma}{x_i}} \right)^{\beta-1} - 1 \right)}}{x_i \left(1 - e^{-\lambda \left(\left(1 - e^{-\frac{a\gamma}{x_i}} \right)^{\beta-1} - 1 \right)} \right)}.$$

Hence, the MLE for each parameter is produced by equating the aforementioned equations to zero and numerically solving them using the optimization technique in R-package.

5. Numerical study

In this section, a numerical study is provided to analyze the performance of the OEKIE's MLEs. Samples of sizes 25, 50, 100, and 500 were generated from the OEKIE distribution for three sets with various parameter values, as shown below:

Set 1: $(\lambda = 2.9, \alpha = 2.5, a = 0.7, \beta = 3.5, \gamma = 0.9)$,
Set 2: $(\lambda = 0.5, \alpha = 0.7, a = 1.9, \beta = 0.9, \gamma = 1.2)$,
Set 3: $(\lambda = 1.5, \alpha = 0.2, a = 2.0, \beta = 2.0, \gamma = 2.0)$.

Average estimates of OEKIE's parameters and their mean squared errors (MSE) are calculated for each sample size. Table 1 shows that the MSE decreases as the sample size n increases and the MLEs of the parameters become closer to their true values.

Table 1: Numerical study of the OEKIE distribution

		Set 1		Set 2		Set 3	
n	Par.	MLEs	MSE	MLEs	MSE	MLEs	MSE
25	λ	6.6681	15.2186	1.0496	3.3760	1.3233	5.7364
	α	6.1210	12.2211	0.8981	2.5452	0.9551	0.9299
	a	0.8677	0.9247	3.5408	5.3340	2.0585	0.8525
	β	9.1417	23.5833	2.6265	3.6321	1.7205	1.9541
	γ	1.1590	1.3496	3.6012	6.0135	1.7361	0.9911
50	λ	4.9985	8.9745	0.6001	1.2064	1.2473	2.5038
	α	4.4263	6.0000	0.7682	0.9370	0.9534	0.9070
	a	0.7476	0.4533	2.7226	2.9601	2.0559	0.8151
	β	6.5498	18.7188	1.6932	1.6045	1.5988	1.3992
	γ	1.0330	0.7387	2.5429	3.4998	1.6963	0.8038
100	λ	3.7751	3.9615	0.5209	0.4242	1.1695	2.1053
	α	.2728	2.9033	0.7019	0.5567	0.9507	0.9039
	a	0.7362	0.3496	2.5337	2.2951	2.0503	0.8098
	β	5.0486	7.1626	1.2962	0.8365	1.5642	1.1108
	γ	0.9585	0.5374	1.8862	1.7323	1.6889	0.7460
500	λ	3.2220	1.9019	0.4903	0.1472	1.4159	0.0841
	α	2.7260	1.0852	0.7087	0.2831	0.1854	0.0146
	a	0.7033	0.1250	2.0545	0.7350	2.0012	0.0012
	β	3.6171	1.1750	0.9780	0.2588	2.1232	0.1232
	γ	0.8934	0.1704	1.3395	0.6190	2.0752	0.0752

6. COVID-19 applications

The efficacy of OEKIE is investigated by examining four COVID-19 mortality rate data from Saudi Arabia, Canada, Italy, and Mexico. The data are listed as follows.

6.1. COVID-19 mortality rate data in Saudi Arabia

The following (Table 2) are the mortality rate data in Saudi Arabia for 61 days from 1/11/2020 to 31/12/2020, which are obtained from https://covid19.moh.gov.sa/.

Table 2: Mortality rate data in Saudi Arabia

4.4619	4.0169	3.5211	4.0000	3.8991	4.6683	4.1322	4.8469	3.6093
3.5533	4.8232	4.5351	4.5845	5.2459	6.3123	4.4199	6.2069	5.6426
6.6434	7.2398	8.4821	6.9264	5.9524	4.2945	4.6584	5.6291	5.9091
6.4516	5.1724	4.1825	4.8193	4.7826	4.2735	7.3684	5.8824	5.7416
6.2176	8.1761	7.0922	6.5476	7.8313	8.6331	8.8000	7.0423	6.1111
6.0773	5.7471	6.9620	6.1728	5.3571	4.4199	5.0847	5.8201	5.0562
4.9080	5.8442	9.2437	5.3691	8.8496	6.4286	5.1095		

6.2. COVID-19 mortality rate data in Canada

The following (Table 3) are the mortality rate data in Canada for 36 days, from 10/4/2020 to 15/5/2020 [https://covid19.who.int/], and was studied by Almetwally et al. (2021).

Table 3: Mortality rate data in Canada

3.1091	3.3825	3.1444	3.2135	2.4946	3.5146	4.9274	3.3769	6.8686
3.0914	4.9378	3.1091	3.2823	3.8594	4.0480	4.1685	3.6426	3.2110
2.8636	3.2218	2.9078	3.6346	2.7957	4.2781	4.2202	1.5157	2.6029
3.3592	2.8349	3.1348	2.5261	1.5806	2.7704	2.1901	2.4141	1.9048

6.3. COVID-19 mortality rate in Italy Data

The following (Table 4) are the mortality rate data in Italy for 59 days, from 27/2/2020 to 27/4/2020 [https://covid19.who.int/], and was studied by Almongy et al. (2021).

Table 4: Mortality rate data in Italy

4.571	7.201	3.606	8.479	11.410	8.961	10.919	10.908	6.503
18.474	11.010	17.337	16.561	13.226	15.137	8.697	15.787	13.333
11.822	14.242	11.273	14.330	16.046	11.950	10.282	11.775	10.138
9.037	12.396	10.644	8.646	8.905	8.906	7.407	7.445	7.214
6.194	4.640	5.452	5.073	4.416	4.859	4.408	4.639	3.148
4.040	4.253	4.011	3.564	3.827	3.134	2.780	2.881	3.341
2.686	2.814	2.508	2.450	1.518				

6.4. COVID-19 mortality rate data in Mexico

The following (Table 5) are the mortality rate data in Mexico for 108 days, from 4/3/2020 to 20/7/2020 [https://covid19.who.int/], and was studied by Almongy et al. (2021):

Table 5: Mortality rate data in Mexico

8.826	6.105	10.383	7.267	13.220	6.015	10.855	6.122	10.685
10.035	5.242	7.630	14.604	7.903	6.327	9.391	14.962	4.730
3.215	16.498	11.665	9.284	12.878	6.656	3.440	5.854	8.813
10.043	7.260	5.985	4.424	4.344	5.143	9.935	7.840	9.550
6.968	6.370	3.537	3.286	10.158	8.108	6.697	7.151	6.560
2.988	3.336	6.814	8.325	7.854	8.551	3.228	3.499	3.751
7.486	6.625	6.140	4.909	4.661	1.867	2.838	5.392	12.042
8.696	6.412	3.395	1.815	3.327	5.406	6.182	4.949	4.089
3.359	2.070	3.298	5.317	5.442	4.557	4.292	2.500	6.535
4.648	4.697	5.459	4.120	3.922	3.219	1.402	2.438	3.257
3.632	3.233	3.027	2.352	1.205	2.077	3.778	3.218	2.926
2.601	2.065	1.041	1.800	3.029	2.058	2.326	2.506	1.923

The basic statistics for the four COVID-19 mortality rate data in Saudi Arabia, Canada, Italy, and Mexico are reported in Table 6.

The significant distinctions between the four COVID-19 mortality rate statistics are in their central and dispersion features and their skewness characteristics. The mean and median of COVID-19 mortality rate data in Italy are the highest, while Canada's mortality rate data is more skewed to the right compared to other countries' mortality rates. The descriptive statistics are strengthened in Fig. 5 by presenting the total time on test (TTT) plots, which are used to determine the shape of the hrf of such data (Aarset, 1987).

Table 6: Statistics for COVID-19 mortality rate data

Data	Size	Median	Mean	Standard Deviation	Skewness	Kurtosis
Saudi Arabia	61	5.6426	5.7343	1.4258	0.6461	2.7797
Canada	36	3.1777	3.2816	0.9985	1.2139	6.1516
Italy	59	7.4450	8.1562	4.5267	0.4524	2.1282
Mexico	108	5.1925	5.7581	3.2542	0.9866	3.6813

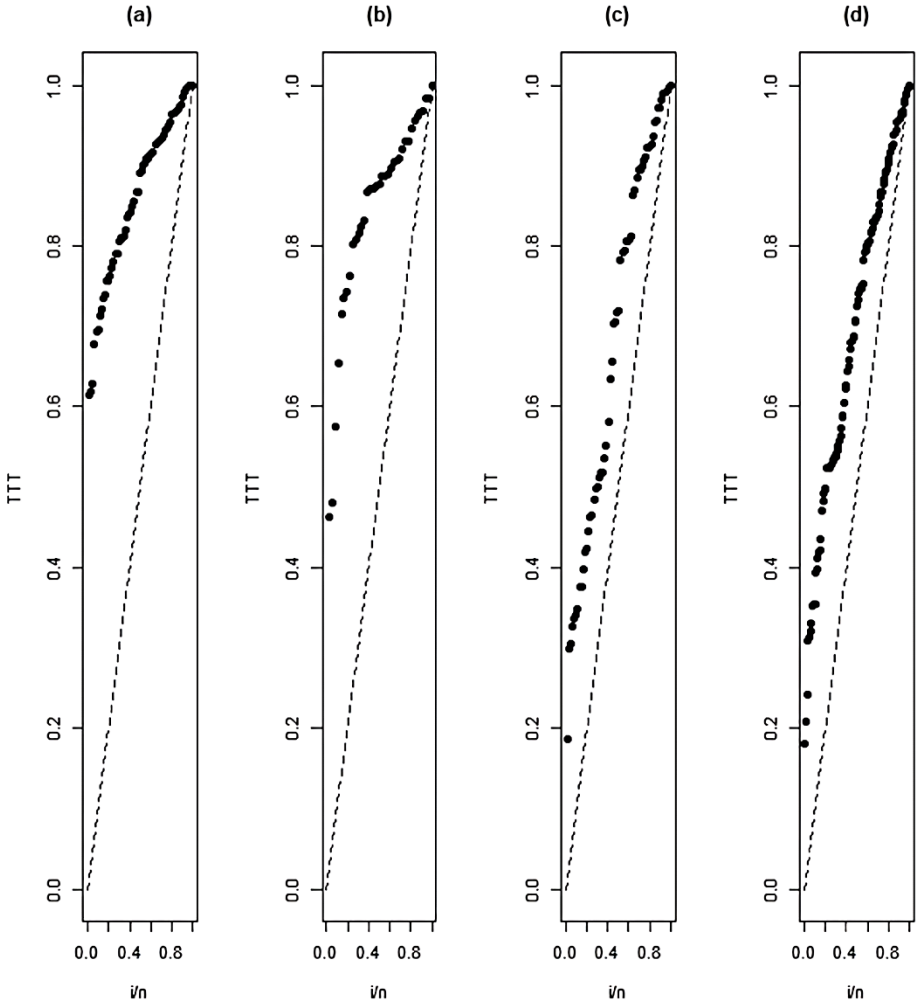

Fig. 5: TTT plots for the COVID-19 mortality rate data in Saudi Arabia (a), Canada (b), Italy (c), and Mexico (d)

The graphs in Fig. 5 show that COVID-19 mortality rate data of all countries have a concave TTT line, indicating monotonic hrf, supporting the suitability of OEKIE to fit these data.

The appropriateness of the COVID-19 mortality rate data for the OEKIE is evaluated by comparing its fit to four competing distributions with CDF as follows:

• The odd Kumaraswamy inverse Weibull (OKIW) by Atem (2018) and Atem et al. (2017):

$$F(x)=\left[1-e^{1-\left(1-e^{-\lambda\left(\frac{\gamma}{x}\right)^{\beta}}\right)^{-\delta}}\right]^{\alpha}.$$

• The Kum-IE by Oguntunde et al. (2017) with CDF given in Eq. 6.

• The Odd generalized exponential inverse-exponential (OEIE) (Yahaya and Abba, 2017):

$$F(x)=\left[1-e^{-\lambda\left(e^{\frac{\gamma}{x}}-1\right)^{-1}}\right]^{\alpha}.$$

• The generalized inverted generalized exponential (GIE) (Oguntunde and Adejumo, 2015)

$$F(x)=1-\left(1-e^{-\left(\frac{\gamma}{x}\right)^{b}}\right)^{\beta}.$$

The goodness of fit criteria (GoF) such as the $-\ell$, Akaike information criterion (AIC), corrected AIC (CAIC), Bayesian information criterion (BIC), Kramér-von Mises (W*), Anderson-Darling (AD*), Kolmogorov-Smirnov (KS) and p-value statistics are obtained to evaluate the OEKIE performance. In general, a superior fit to the data is achieved when the value of these statistics is less than that of competing fits. The MLEs, along with the GoF criteria measures of OEKIE and competing distributions for the four COVID-19 mortality rate data sets are reported in Tables 7-10. In addition, Figs. 6-9 compare the estimated pdf and cdf of OEKIE to competing distributions for the four COVID-19 data sets.

Table 7: MLEs and GoF measures for the COVID-19 mortality rate data in Saudi Arabia.

Distributions	OEKIE	OKIW	Kum-IE	OEIE	GIE
Estimates	$\hat{\lambda} = 4.5623$	$\hat{\lambda} = 8.5038$	$\hat{a} = 6.2407$	$\hat{\lambda} = 40.9055$	$\hat{\beta} = 299.2887$
	$\hat{\alpha} = 9.4283$	$\hat{\alpha} = 8.6102$	$\hat{\beta} = 21.3358$	$\hat{\alpha} = 0.9706$	$\hat{\gamma} = 35.3393$
	$\hat{a} = 1.9642$	$\hat{a} = 0.6916$	$\hat{\gamma}$ =3.0396	$\hat{\gamma} = 23.8904$	
	$\hat{b} = 1.2060$	$\hat{\delta} = 3.6127$			
	$\hat{\gamma} = 3.2379$	$\hat{\gamma}$ =0.3349			
$-\ell$	104.2425	104.6963	109.5656	111.4505	111.5288
AIC	218.4849	219.3926	225.1311	228.9010	227.0576
CAIC	223.7621	224.6697	228.2974	232.0673	229.1684
BIC	229.0393	229.9469	231.4637	235.2336	231.2793
W*	0.0296	0.0316	17.2824	0.1753	0.3917
AD*	0.2105	0.2708	87.0993	0.9725	3.0710
KS	0.0581	0.0596	0.9467	0.1037	0.1604
p-value	0.9861	0.9819	0.5139	0.5270	0.0866

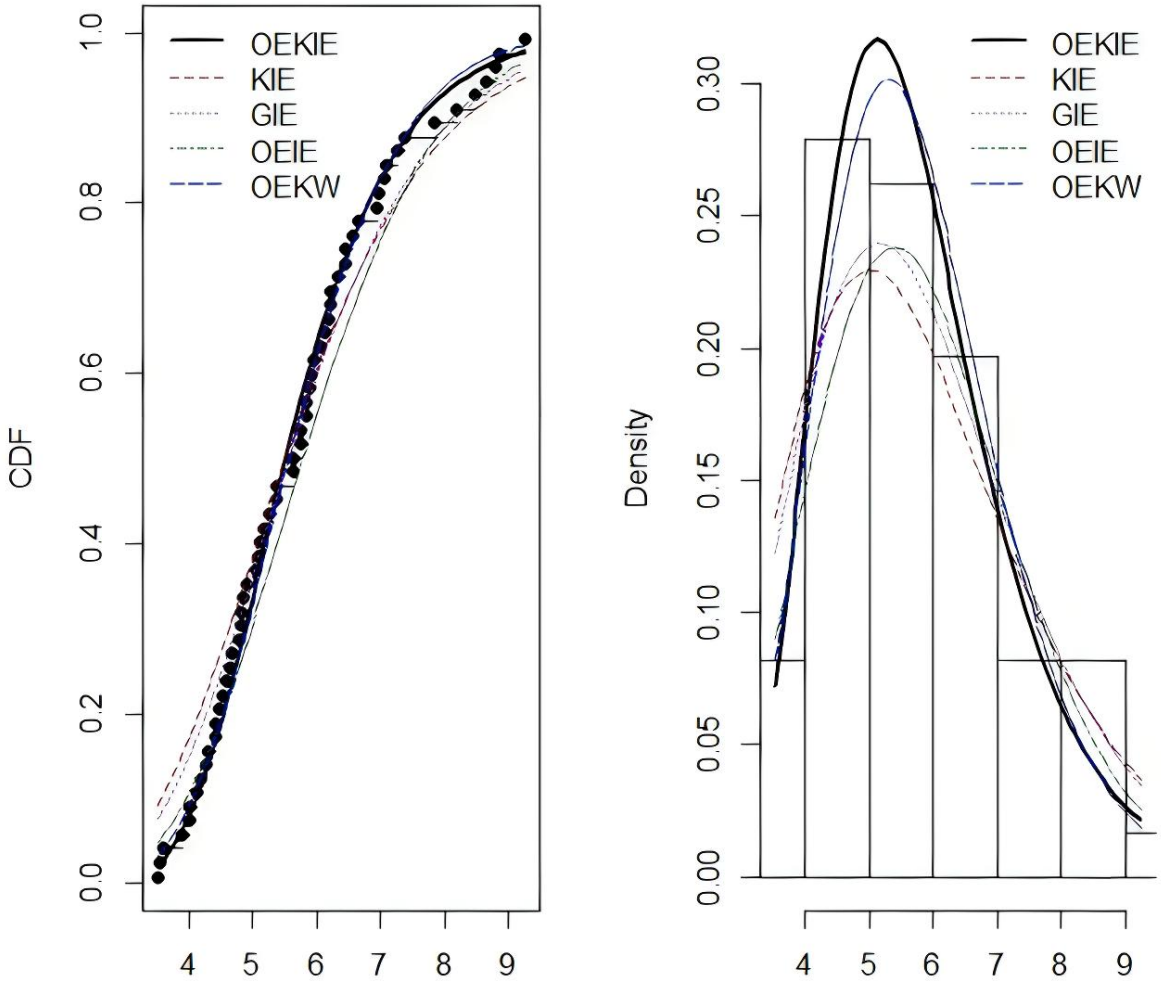

Fig. 6: Estimated CDFs and pdfs for COVID-19 mortality rate data in Saudi Arabia

Table 8: MLEs and GoF measures for COVID-19 mortality rate data in Canada

Distributions	OEKIE	OKIW	Kum-IE	OEIE	GIE
Estimates	$\hat{\lambda} = 0.0517$	$\hat{\lambda} = 5.3100$	$\hat{a} = 7.7390$	$\hat{\lambda} = 23.6590$	$\hat{\beta} = 162.5989$
	$\hat{\alpha} = 8.1034$	$\hat{\alpha} = 4.8644$	$\hat{\beta} = 2.4013$	$\hat{\alpha} = 0.7944$	$\hat{\gamma} = 17.9672$
	$\hat{a} = 1.7592$	$\hat{a} = 0.5447$	$\hat{\gamma}$ =0.5530	$\hat{\gamma} = 12.3121$	
	$\hat{\beta} = 1.5439$	$\hat{\delta} = 6.1207$			
	$\hat{\gamma} = 0.1502$	$\hat{\gamma} = 0.4429$			
$-\ell$	48.0964	48.3186	65.6005	53.0433	54.1811
AIC	106.1930	106.8712	137.2011	112.7785	112.332
CAIC	110.1518	110.8300	113.9155	115.1538	113.915
BIC	114.1106	114.7887	141.9517	117.5290	115.499
W*	0.0900	0.1088	0.8799	0.1819	0.1280
AD*	0.5307	0.6149	4.7880	0.9723	1.3203
KS	0.1058	0.1305	0.2492	0.1440	0.1419
p-value	0.8142	0.5710	0.0227	0.4438	0.4627

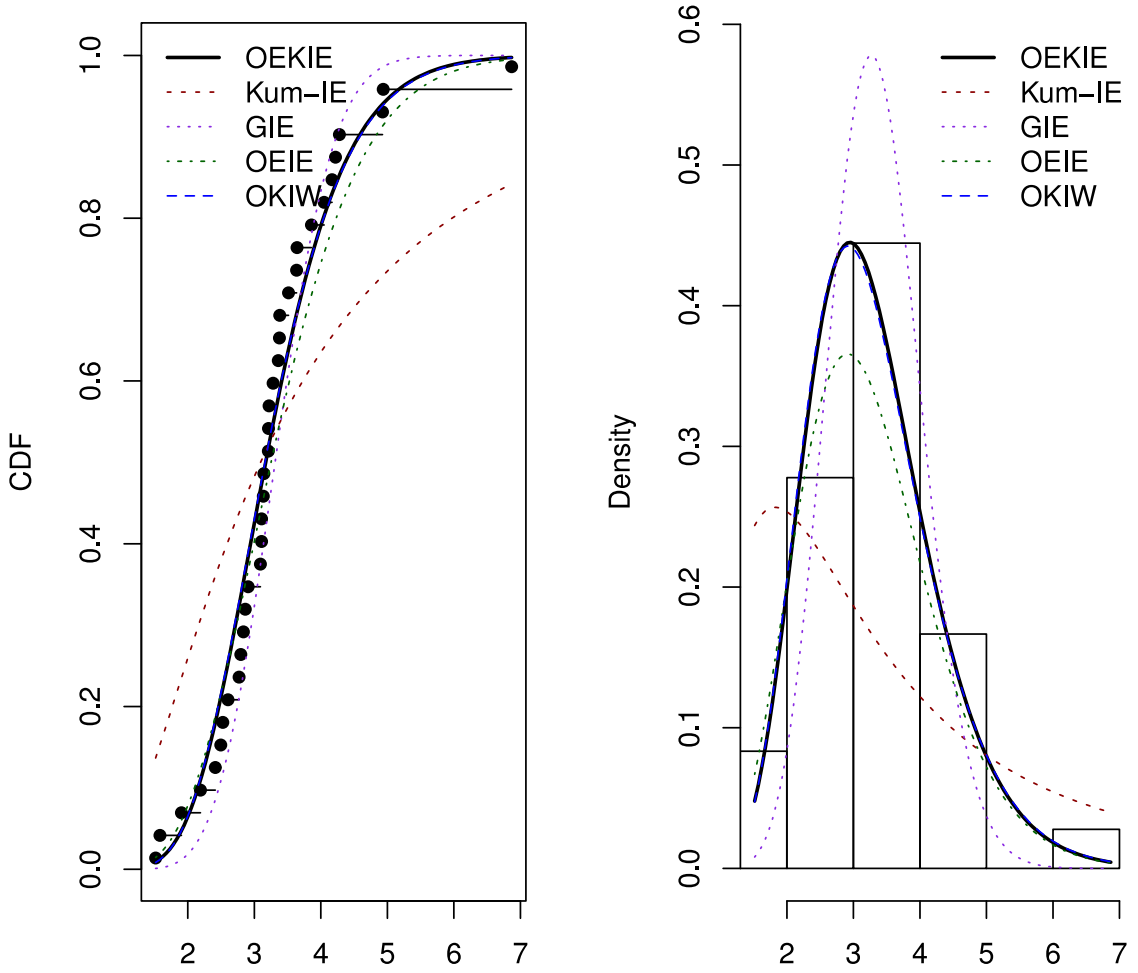

Fig. 7: Estimated CDFs and pdfs for COVID-19 mortality rate data in Canada

Table 9: MLEs and GoF measures for the COVID-19 mortality rate data in Italy

Distributions	OEKIE	OKIW	Kum-IE	OEIE	GIE
Estimates	$\hat{\lambda} = 0.2135$	$\hat{\lambda} = 6.5617$	$\hat{a} = 3.3417$	$\hat{\lambda} = 21.5765$	$\hat{\beta} = 3.3731$
	$\hat{\alpha} = 0.1946$	$\hat{\alpha} = 0.1796$	$\hat{\beta} = 3.3719$	$\hat{\alpha} = 0.1574$	$\hat{\gamma} = 11.0133$
	$\hat{a} = 6.0991$	$\hat{a} = 0.9605$	$\hat{\gamma}$ =3.2946	$\hat{\gamma} = 52.8179$	
	$\hat{b} = 21.0211$	$\hat{\delta} = 20.1175$			
	$\hat{\gamma} = 6.2931$	$\hat{\gamma}$ =7.4960			
$-\ell$	163.2078	164.0031	170.6591	168.3111	170.6591
AIC	336.4155	338.0062	347.3182	342.6222	345.3182
CAIC	341.6094	343.2001	350.4345	345.7385	347.3957
BIC	346.8032	348.3939	353.5508	348.8548	349.4733
W*	0.0551	0.1056	0.2422	0.1033	0.2422
AD*	0.3264	0.5636	1.3456	0.6162	1.3457
KS	0.0881	0.0933	0.1501	0.0980	0.1501
p-value	0.7159	0.6149	0.1259	0.5878	0.1262

Table 10: MLEs and GoF measures for the COVID-19 mortality rate data in Mexico

Distributions	OEKIE	OKIW	Kum-IE	OEIE	GIE
Estimates	$\hat{\lambda} = 2.3161$	$\hat{\lambda} = 12.1937$	$\hat{a} = 1.5753$	$\hat{\lambda} = 26.6543$	$\hat{\beta} = 3.9349$
	$\hat{\alpha} = 0.2544$	$\hat{\alpha} = 10.5343$	$\hat{\beta} = 3.9346$	$\hat{\alpha} = 0.1731$	$\hat{\gamma} = 8.5998$
	$\hat{a} = 9.0234$	$\hat{a} = 0.3018$	$\hat{\gamma}$ =5.4485	$\hat{\gamma} = 36.9258$	
	$\hat{b} = 4.1073$	$\hat{\delta} = 3.5912$			
	$\hat{\gamma} = 2.7844$	$\hat{\gamma}$ =0.0020			
$-\ell$	264.823	268.3603	269.3388	268.7825	269.3382
AIC	539.6460	546.7206	544.6777	543.5650	542.6764
CAIC	546.3513	553.4259	548.7009	547.5882	545.3585
BIC	553.0567	560.1313	552.7241	551.6114	548.0407
W*	0.0322	0.3099	0.1425	0.0326	0.1381
AD*	0.1910	1.8060	0.8216	0.1900	0.8059
KS	0.0517	0.1182	0.0925	0.0530	0.0914
p-value	0.9348	0.0977	0.3130	0.9218	0.3274

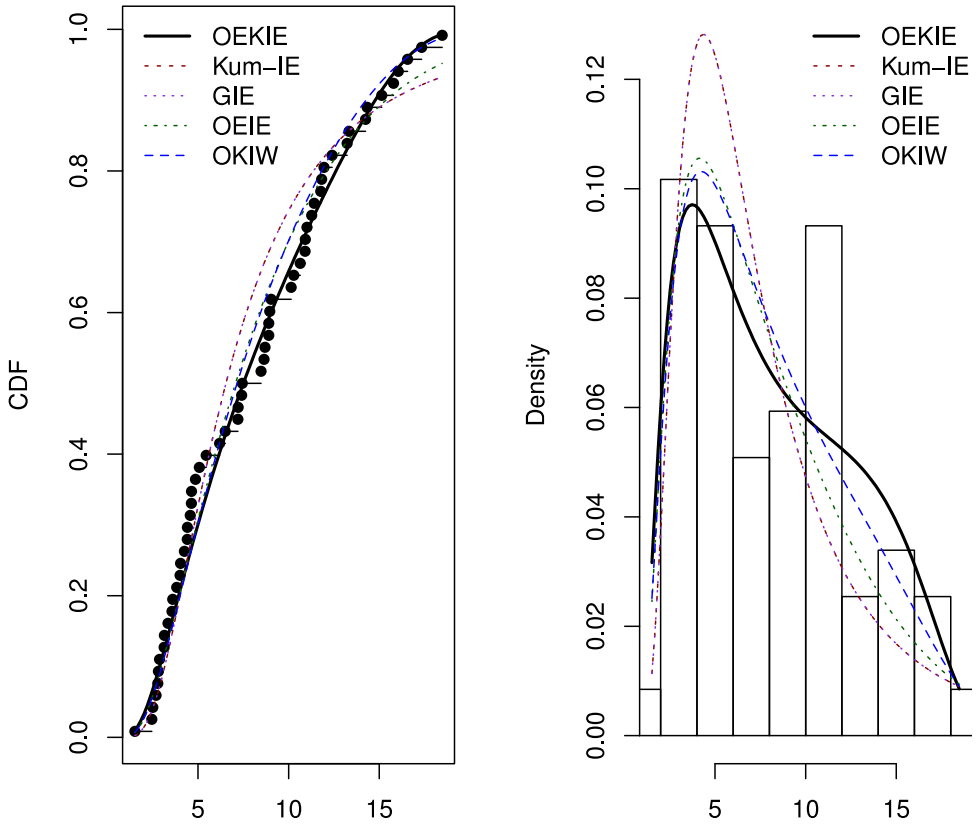

Fig. 8: Estimated CDFs and pdfs for COVID-19 mortality rate data in Italy

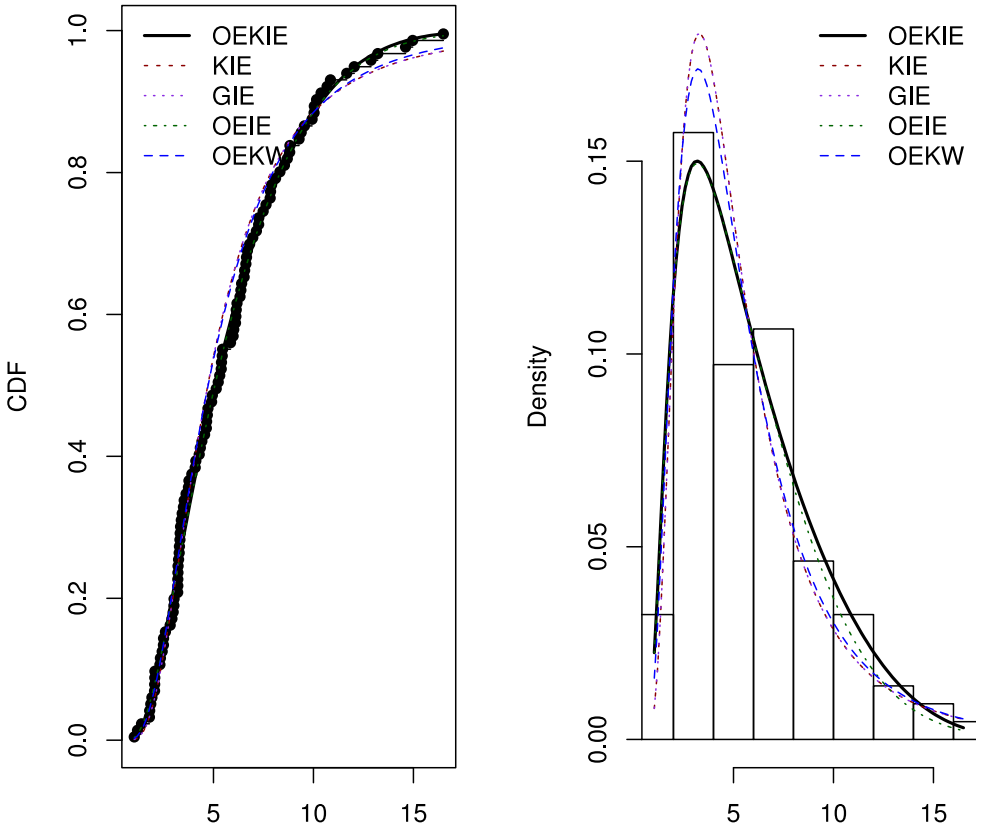

Fig. 9: Estimated CDFs and pdfs for COVID-19 mortality rate data in Mexico

Referring to Tables 7-10, the OEKIE has the lowest values of ℓ, AIC, CAIC, BIC, and K-S statistics and the highest p-value among all distributions. This indicates that, when compared to other competing distributions, the OEKIE gives better fits for COVID-19 mortality rate data from Saudi Arabia, Canada, Italy, and Mexico. Moreover, it is evident from Fig. 6-Fig. 9 that the OEKIE fits the histogram of COVID-19 mortality rate data from all four countries better than other competing distributions.

7. Conclusion

This article developed the OEKIE distribution based on combining the odd generalized exponential generator with the Kum-G family. The OEKIE offers greater versatility since its density and hrf have attractive shapes for fitting a wide range of real-world data behaviors. The main mathematical characteristics are derived, and the statistical modeling capability is examined. The well-established ML technique is used to estimate OEKIE's parameters. The OEKIE model's efficiency is assessed by its applications to four COVID-19 data sets from Saudi Arabia, Canada, Italy, and Mexico. The study's main notable finding is that OEKIE outperforms competing distributions in terms of performance and adaptability. The OEKIE has the lowest GoF criterion and highest p-value of the KS statistics for the four COVID-19 mortality rate data sets.

Compliance with ethical standards

Conflict of interest

The author(s) declared no potential conflicts of interest with respect to the research, authorship, and/or publication of this article.

References

Aarset MV (1987). How to identify a bathtub hazard rate? IEEE Transactions on Reliability, 36(1): 106-108. https://doi.org/10.1109/TR.1987.5222310

Abouammoh AM and Alshingiti AM (2009). Reliability estimation of generalized inverted exponential distribution. Journal of Statistical Computation and Simulation, 79(11): 1301-1315. https://doi.org/10.1080/00949650802261095

Almetwally EM, Alharbi R, Alnagar D, and Hafez EH (2021). A new inverted Topp-Leone distribution: Applications to the COVID-19 mortality rate in two different countries. Axioms, 10(1): 25. https://doi.org/10.3390/axioms10010025

Almongy HM, Almetwally EM, Aljohani HM, Alghamdi AS, and Hafez EH (2021). A new extended Rayleigh distribution with applications of COVID-19 data. Results in Physics, 23: 104012. https://doi.org/10.1016/j.rinp.2021.104012 **PMid:33728260 PMCid:PMC7952137**

Alzaatreh A, Lee C, and Famoye F (2013). A new method for generating families of continuous distributions. METRON, 71(1): 63-79. https://doi.org/10.1007/s40300-013-0007-y

Atem BAM (2018). On the odd Kumaraswamy inverse Weibull distribution with application to survival data. Ph.D. Dissertation, Jomo Kenyatta University of Agriculture and Technology, Juja, Kenya.

Atem BAM, Orwa GO, and Mbugua LN (2017). The odd Kumaraswamy inverse Weibull distribution with application to survival data. Advances and Applications in Statistics, 51: 309-335. https://doi.org/10.17654/AS051050309

Bantan RA, Chesneau C, Jamal F, and Elgarhy M (2020). On the analysis of new COVID-19 cases in Pakistan using an exponentiated version of the M family of distributions. Mathematics, 8(6): 953. https://doi.org/10.3390/math8060953

Bourguignon M, Silva RB, and Cordeiro GM (2014). The Weibull-G family of probability distributions. Journal of Data Science, 12(1): 53-68. https://doi.org/10.6339/JDS.201401_12(1).0004

Cordeiro GM and de Castro M (2011). A new family of generalized distributions. Journal of Statistical Computation and Simulation, 81(7): 883-898. https://doi.org/10.1080/00949650903530745

Cordeiro GM, Afify AZ, Yousof HM, Pescim RR, and Aryal GR (2017). The exponentiated Weibull-H family of distributions: Theory and applications. Mediterranean Journal of Mathematics, 14(4): 1-22. https://doi.org/10.1007/s00009-017-0955-1

Eugene N, Lee C, and Famoye F (2002). Beta-normal distribution and its applications. Communications in Statistics-Theory and Methods, 31(4): 497-512. https://doi.org/10.1081/STA-120003130

Jones MC (2009). Kumaraswamy's distribution: A beta-type distribution with some tractability advantages. Statistical Methodology, 6(1): 70–81. https://doi.org/10.1016/j.stamet.2008.04.001

Keller AZ, Kamath ARR, and Perera UD (1982). Reliability analysis of CNC machine tools. Reliability Engineering, 3(6): 449-473. https://doi.org/10.1016/0143-8174(82)90036-1

Kumaraswamy P (1980). A generalized probability density function for double-bounded random processes. Journal of Hydrology, 46(1–2): 79–88. https://doi.org/10.1016/0022-1694(80)90036-0

Lemonte AJ (2013). A new exponential-type distribution with constant, decreasing, increasing, upside-down bathtub and bathtub-shaped failure rate function. Computational Statistics and Data Analysis, 62: 149-170. https://doi.org/10.1016/j.csda.2013.01.011

Lin CT, Duran BS, and Lewis TO (1989). Inverted gamma as a life distribution. Microelectronics Reliability, 29(4): 619-626. https://doi.org/10.1016/0026-2714(89)90352-1

Mohamed H, Abo-Hussien AE, Mousa SA, and Ismail MM (2021). The analysis for the recovery cases of COVID-19 in Egypt using odd generalized exponential Lomax distribution. Journal of Advances in Mathematics and Computer Science, 36(5): 52-65. https://doi.org/10.9734/jamcs/2021/v36i530363

Mohammed AS and Yahaya A (2019). Exponentiated transmuted inverse exponential distribution with application. Annals of Statistical Theory and Applications, 2: 71-80.

Moors JJA (1988). A quantile alternative for kurtosis. Journal of the Royal Statistical Society: Series D (The Statistician), 37(1): 25-32. https://doi.org/10.2307/2348376

Oguntunde PE and Adejumo AO (2015). The generalized inverted generalized exponential distribution with an application to a censored data. Journal of Statistics Applications and Probability, 4(2): 223-230.

Oguntunde PE, Adejumo A, and Balogun OS (2014). Statistical properties of the exponentiated generalized inverted exponential distribution. Applied Mathematics, 4(2): 47-55.

Oguntunde PE, Adejumo A, and Owoloko EA (2017). Application of Kumaraswamy inverse exponential distribution to real lifetime data. International Journal of Applied Mathematics and Statistics, 56(5): 34–47.

Tahir MH, Cordeiro GM, Alizadeh M, Mansoor M, Zubair M, and Hamedani GG (2015). The odd generalized exponential family of distributions with applications. Journal of Statistical Distributions and Applications, 2: 1. https://doi.org/10.1186/s40488-014-0024-2

Yahaya A and Abba B (2017). Odd generalized exponential inverse-exponential distribution with its properties and application. Journal of the Nigerian Association of Mathematical Physics, 41: 297-304.